PCCP

Accepted Manuscript

ROYAL SOCIETY OF CHEMISTRY

www.rsc.org/pccp

Journal Name

ARTICLE

Interactions of a biocompatible water-soluble anthracenyl polymer derivative with double-stranded DNA

Received 01st September 2015,
Accepted 00th January 20xx

DOI: 10.1039/x0xx00000x

www.rsc.org/

Marco Deiana[a], Bastien Mettra[b], Katarzyna Matczyszyn[a]*, Katarzyna Piela[c], Delphine Pitrat[b], Joanna Olesiak-Banska[a], Cyrille Monnereau[b], Chantal Andraud[b], Marek Samoc[a]

ABSTRACT. We have studied the interaction of a polymeric water soluble anthracenyl derivative (**Ant-PHEA**) with salmon testes DNA. The results from UV-Vis, fluorescence, Fourier transform infrared (FT-IR) and circular dichroism spectroscopies indicate that the groove binding process regulates the interaction between **Ant-PHEA** and DNA. The binding constants, calculated by absorption spectroscopy at 298, 304 and 310 K, were equal to 3.2×10^5 M^{-1}, 4.7×10^5 M^{-1}, and 6.6×10^5 M^{-1} respectively, proving a relative high affinity of **Ant-PHEA** towards salmon testes DNA. Results of Hoechst 33258 displacement assays strongly support the groove binding mode of **Ant-PHEA** to DNA. The association stoichiometry of the **Ant-PHEA**:DNA adduct was found to be 1 every 5 base pairs. FT-IR spectra, recorded at different **Ant-PHEA**/DNA molar ratios, indicate the involvement of the phosphate groups and adenine and thymine DNA bases in the association process. Thermodynamic results suggest that hydrophobic forces regulate the binding of **Ant-PHEA** with DNA without excluding some extent of involvment of van der Waals forces and hydrogen bonding arising due to surface binding between the hydrophilic polymeric arms of the ligand and the functional groups positioned on the edge of the groove. The resulting composite biomaterial could constitute a valuable candidate for future biological and/or photonic applications.

Introduction

Biocompatible chromophores used for bio-related two-photon applications such as fluorescence microscopy imaging and photo-dynamic therapy (PDT) have been object of much attention in recent years.[1-4] It has been shown that, common stains used for biological applications such as ethidium bromide and Hoechst 33342 do not present high two-photon absorption,[5,6] since usually, good non-linear photon absorbers present a large π-conjugated skeleton making them highly hydrophobic and thus not suitable for applications in aqueous systems.[7] In this context, Monnereau et al[8,9] developed a new strategy that makes such molecules water-soluble and biocompatible allowing the involvement with bio systems, while preserving the photo-physical properties of their lipophilic precursors, including two-photon absorption and emission properties. In this context, there is special interest in molecules that can interact with DNA, especially those that show a tendency to bind in a sequence-specific manner. Beside the use of such molecules as specific biological probes, the advent of DNA as a photonic material makes it interesting to consider DNA-dye complexes as components for the construction of bio-sourced composite optoelectronic materials and devices.[10-14] Fabrication of such devices requires a large compatibility between the DNA substrate and the dye.[15] Thus, the search of agents with a large association constant and a high selectivity is one of the primary goals in these area.[16-21] To achieve these properties, efforts have been undertaken to modify the structural characteristics of the ligand and to evaluate the conformational changes induced in DNA upon binding.[22,23] Moreover, the structural changes generated by the binding interaction with external compounds make DNA a target molecule for antiviral and anticancer therapies.[24-27] DNA can interact with guest molecules mainly in three different ways: intercalation, groove binding and external binding.[16] Intercalation occurs when the planar polycyclic aromatic molecules are inserted between two base pairs. This induces significant conformational changes in the DNA structure and is generally independent of base-pair sequence.[28] Typical binding constants found for well-known intercalators such as Methylene Blue-DNA (K_a= 2.13×10^4 M^{-1}), Acridine Orange-DNA (K_a= 2.69×10^4) and Ethidium Bromide-DNA (K_a= $6.58\times10^4 M^{-1}$) have a magnitude of 10^4 M^{-1} .[27] Groove binding molecules are typically constituted by at least two aromatic rings and must be flexible to fit perfectly into the groove. Minor groove binders usually involve greater binding affinity and higher sequence specificity than that of intercalators. Since the binding pocket of the DNA groove is defined by two different regions, namely the bottom formed by the edges of the nucleic bases and the walls formed by the deoxyribose-phsophate backbone, the ligand-DNA association process is mainly driven by a combination of hydrophobic, van der Waals, electrostatic and hydrogen-bonding interactions.[24,28] As the DNA minor groove presents a unique pattern of hydrogen bond

[a] Advanced Materials Engineering and Modelling Group, Faculty of Chemistry, Wroclaw University of Technology, Wyb. Wyspianskiego 27, 50-370 Wroclaw (Poland)
[b] Laboratoire de Chimie, CNRS UMR 5182, Ecole Normale Supérieure de Lyon, Université Lyon 1, Lyon, (France)
[c] Department of Physical and Quantum Chemistry, Faculty of Chemistry, Wroclaw University of Technology, Wyb. Wyspianskiego 27, 50-370 Wroclaw (Poland)

donors and acceptors specific functional groups along the ligand moiety are often required to enhance the binding orientation.[29,30] In addition, electrostatic forces may play an important role for minor groove binders even so, such binding mode has been demonstrated for neutral, mono-charged and multicharged ligands.[28] Anyway, the right insertion of positive charges and electronegative atoms along the guest molecule template can enhance the specificity and affinity of the ligands for the duplex.[29] The binding constant associated with such interactions ranges from 10^5 to 10^9 M^{-1}.[24] The third mode, called external binding, it is usually referred to molecules that are not well suited for intercalation or groove binding and it results from attractive electrostatic interactions between positive charges from the ligand and negative charges from the phosphonates of the DNA backbone. The binding constants for external DNA binders are much smaller and are on the order of 10^2 M^{-1}.[31]

A number of studies have indicated that anthracene derivatives bind to DNA mainly through intercalation or groove binding and that the nature of the substituents affects substantially the type of interaction.[32]

The aim of this study was to determine the binding mode and the interaction strength of a 6 units/chain anthracenyl polymer derivative, denoted as **Ant-PHEA** (Fig. 1), to double-stranded salmon sperm DNA. **Ant-PHEA** consists of a highly fluorescent anthracene core specifically designed to display enhanced two-photon fluorescence properties, and four hydrophilic polymeric arms that ensure its biocompatibility. It was thus particularly interesting to investigate the influence of this polymeric structure on the binding mode of the probe. For this purpose we studied different **Ant-PHEA**/DNA compositions, in sodium cacodylate buffer solutions (pH=7.25), by using various complementary spectroscopic techniques (UV-Vis, fluorescence, circular dichroism and FT-IR). It is important to note that the **Ant-PHEA** molecule at physiological pH is neutral (pKa of protonated alcohol and protonated carbonyl are in the range of -3 and -7 respectively, and hence impossible to protonate in aqueous media).

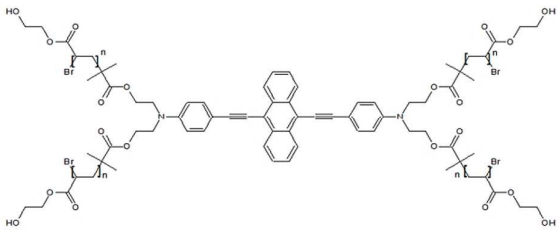

Fig. 1 Chemical structure of **Ant-PHEA** (n=6).

MATERIALS AND METHODS

Apparatus

The UV-Vis absorption spectra were recorded on a Perkin Elmer Lambda 20 UV-Vis spectrometer. An electronic thermostated water bath (PTP-1 Peltier system DBS) was used for controlling the temperature. Fluorescence analyses were carried out with a Hitachi F-4500 spectrofluorometer equipped with a xenon lamp and a thermostat bath. Circular dichroism spectra were recorded with a Jasco J-815 spectropolarimeter (Jasco Inc, USA) equipped with the Jasco Peltier-type temperature controller (CDF-426S/15). All measurements were carried out in 1.0 cm path length quartz cells. The infrared spectra were collected, on the diamond crystal surface under vacuum (< 1 hPa), using a Bruker Vertex70v FT-IR spectrometer. A Metrohm 902 Titrando digital pH meter, equipped with Tiamo 2.3 software, was used to detect the pH values of the solutions.

Reagents and preparation of stock solutions

Common reagent-grade chemicals were used without further purification. The stock solution of deoxyribonucleic acid sodium salt from salmon testes (DNA), purchased from Sigma Aldrich Chem. Co., was prepared by dissolving an appropriate amount of solid DNA powder in 50 mM sodium cacodylate buffer (pH 7.25). Stock solution was stored at 4 °C for 24 hours with occasional stirring and was used after no more than 3 days. The appropriate DNA solution concentrations were determined by absorption spectrometry according to the absorbance at 260 nm. The purity of the DNA was checked by monitoring the ratio of the absorbance at 260 and 280 nm and at 260 and 230 nm giving values higher than 1.8 and 2.2, respectively, thus showing DNA being sufficiently free from protein impurities.[33,34] The **Ant-PHEA** stock solution was prepared dissolving appropriate amounts of the molecule (which synthesis has been reported previously)[8] in a double distilled water to a final concentration of 4.75 mM. The stock solutions were stored protected from light by wrapping the vials with aluminum foil.

UV-Vis measurements

The UV-Vis absorption spectra were recorded at three different temperatures (298, 304 and 310 K) keeping the concentration of **Ant-PHEA** constant at 5 μM and adding incremental amounts of DNA. After addition of DNA to the **Ant-PHEA** solution, the resulting system was left to equilibrate at room temperature for 5 minutes and was then subjected to UV-Vis analysis in the 200-800 nm range. The rise of the absorbance at 489 nm was monitored upon increments in DNA concentration. Appropriate cacodylate buffer was used as reference.

Fluorescence measurements

Emission intensity measurements were carried out with fixed amount of DNA and incremental addition of **Ant-PHEA** until saturation was achieved. Conversely, fluorescence spectra were also recorded keeping constant the concentration of the **Ant-PHEA** and titrating the solution with incremental addition of DNA. All the measurements were performed keeping an excitation and emission slit width of 5.0 nm and using a fluorescence free quartz cell of 1 cm path length.

Competition experiment

The competitive interaction between Hoechst 33258 and **Ant-PHEA** with DNA was performed by adding different amounts of **Ant-PHEA** to the Hoechst-DNA solution. Fluorescence spectra of the mixture were recorded in 360-800 nm using an excitation wavelength of 350 nm. Further study of competition between Ethidium Bromide and **Ant-PHEA** was done by adding different amount of **Ant-PHEA** to the EtBr-DNA solution and recording emission in the wavelength range between 550-800 nm using excitation wavelength of 540 nm. The fluorescence emission measurements were made at room temperature, after an equilibration interval of 10 minutes.

Circular dichroism measurements

CD spectra were recorded at 298 and 313 K in the wavelength range of 200-700 nm at different **Ant-PHEA**/DNA ratios and keeping constant the DNA concentration. Before use, the optical chamber of the CD spectrometer was deoxygenated with dry nitrogen and was held under nitrogen atmosphere during the measurements. Each spectrum was averaged from five successive accumulations.

FT-IR spectroscopic measurements

The infrared spectra were measured after 1 h incubation of the salmon testes DNA with **Ant-PHEA** in aqueous solution. All the spectra were recorded via the Attenuated Total Reflection (ATR) method, in the spectral range 4000-400 cm^{-1} with a resolution of 4 cm^{-1} and accumulation of 64 scans, then transformed into absorbance spectra and normalized using OPUS software. The band at 968 cm^{-1}, which is due to deoxyribose C–C stretching vibrations, in difference spectra [(ds-DNA solution + **Ant-PHEA**) – **Ant-PHEA** solution] was used as internal reference. The plots of the relative intensity (R) of several bands of DNA caused by in-plane vibrations of base pairs and the stretching vibration of the PO_2 versus the **Ant-PHEA** concentrations were obtained by carrying out normalization of bands using $R= I_i / I_{968}$ where I_i is the intensity of absorption band at i cm^{-1} for pure salmon testes DNA and its complex with different concentration of **Ant-PHEA**, and I_{968} is the intensity band of the 968 cm^{-1} internal reference band.[35-37]

Melting studies

DNA melting studies were conducted by monitoring the ellipticity values at 245 nm of the salmon sperm DNA in the absence as well as in the presence of **Ant-PHEA** varying the temperature from 20 to 90 °C, with an interval of 2 ^{0}C, in 10 mM sodium cacodylate trihydrate (pH 7.25)**.**[38] The DNA melting temperature (T_m) was determined to be the transition midpoint.

RESULTS AND DISCUSSION

UV-Vis absorption spectra of Ant-PHEA-DNA adducts

Absorption spectral titration is one of the most common method used to determine the binding mode between guest molecules and DNA. The occurrence of interactions between ligands and the DNA helix is usually investigated by following changes in the absorbance and shifts in the wavelength of the selected absorption band.[39-41] Molecules that interact with DNA through intercalation, such as ethidium bromide, give rise to a decrease in absorbance (hypochromism) and a red shift in wavelength (bathochromism) due to the involvement of a stacking interaction between the aromatic chromophore and the DNA base pairs.[42] The extent of hypochromism is generally consistent with the strength of the intercalative interaction.[43] On the other hand, drugs which bind in non-intercalative mode or electrostatically with DNA may give rise either to hyperchromic or hypochromic effects.[44-47]

UV-Vis spectrum of Ant-PHEA displays a main charge transfer (CT) band at 489 nm and additional bands at shorter wavelengths (284 and 256 nm). When DNA is added to **Ant-PHEA** the absorption band at 489 nm is affected and a hyperchromic effect is observed accompanied by a hypsochromic shift of 4 nm (Fig. 2). The coexistence of hyperchromism and hypsochromism could be associated to the surface binding of **Ant-PHEA** with the functional groups of the DNA, located in the major and minor grooves. Similar interaction modes were found for Emodin and Esculetin-DNA systems and a groove binding mode was assigned.[48,49] Thus, on the basis of UV-Vis data, the intercalative binding mode, which typically induces large changes in the absorbance and peak wavelength, can be ruled out. The small variations of the absorption band of **Ant-PHEA**, recorded following the DNA addition suggest that **Ant-PHEA** interacts with DNA by groove binding.[50,51]

The intrinsic association constant (K_a) is a crucial parameter that defines the binding affinity between small molecules and DNA; its magnitude may help to discern between different interaction mechanisms. We calculated the K_a values at three temperatures (298, 304 and 310 K) using the equation:[52]

$$\mathbf{1}/(\mathbf{A}-\mathbf{A_0}) = \mathbf{1}/(\mathbf{A}_\infty - \mathbf{A_0}) + \mathbf{1}/[\mathbf{DNA}]\cdot\mathbf{1}/\mathbf{K_a}(\mathbf{A}_\infty - \mathbf{A_0}) \quad (1)$$

where A_0 and A are the absorbances of **Ant-PHEA** in the absence and in the presence of DNA, respectively, A_∞ is the final absorbance of the **Ant-PHEA**-DNA adduct. The plot of $1/(A-A_0)$ versus $1/C_{DNA}$ is linear and the binding constant can be calculated from the ratio of the intercept and the slope (Inset Fig. 2). The K_a values were found to be 3.2×10^5 M^{-1} (298 K), 4.7×10^5 M^{-1} (304 K) and 6.6×10^5 M^{-1} (310 K). As mentioned before, these K_a values are higher than those found for classical intercalators and external binders indicating that the groove binding is most likely the dominant mode of the interaction between **Ant-PHEA** and DNA.

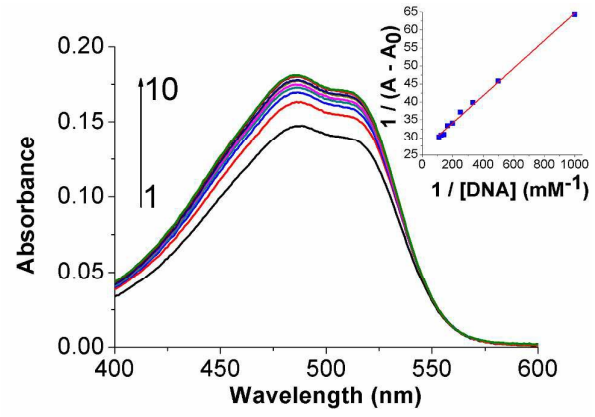

Fig. 2 UV-Vis absorption spectra of **Ant-PHEA** (5 µM) treated with: 0.0, 1.0, 2.0, 3.0, 4.0, 5.0, 6.0 7.0, 8.0 and 9.0 µM (curves 1-10) of DNA at 310 K in 50 mM sodium cacodylate trihydrate (pH 7.25). Inset: Plot of 1/(A-A0) against 1/[DNA] for the **Ant-PHEA**-DNA system at 310 K. A0 and A are the absorbances of **Ant-PHEA** in absence and in presence of DNA.

Spectrofluorimetric studies

The binding of **Ant-PHEA** to DNA was further studied by fluorescence spectroscopy, keeping constant the concentration of **Ant-PHEA** and varying that of DNA. **Ant-PHEA** is a strong fluorophore (Φ_f = 0.62 in water) emitting in the range of 530 – 680 nm with a maximum located at 564 nm.[8]

The incremental addition of DNA to **Ant-PHEA** solution induces a continuous increase in the intensity of the fluorescence band with a slight blue-shift (from 564 nm to 562 nm) indicating that an interaction between **Ant-PHEA** and DNA takes place (Fig. 3). However, the observed magnitude of fluorescence increase is strictly proportional to that observed for the absorption (*vide supra*), indicating that the quantum yield of the bound and unbound molecule remains similar.

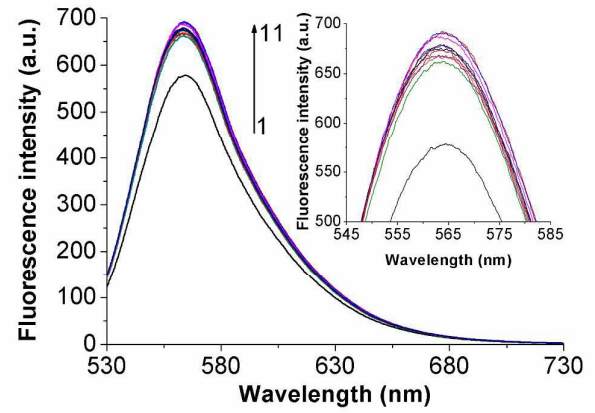

Fig. 3 Fluorescence emission spectra of **Ant-PHEA** (5.0 µM) treated with: 0.0, 1.0, 2.0, 3.0, 4.0, 5.0, 6.0, 7.0, 8.0, 9.0, and 10.0 µM (curves 1-11) of DNA at room temperature (λexc = 516 nm). Inset: Emission spectra detail of **Ant-PHEA** with DNA in the spectral region 545-585 nm.

Determination of the binding mechanism by displacement assay

In order to provide further insights into the mode of binding of **Ant-PHEA** towards the DNA moiety, an additional displacement assay was performed by using Hoechst 33258 as a probe. Hoechst 33258 is a synthetic N-methylpiperazine derivative, which shows a specifical binding affinity for the A-T rich sequences located along the minor grooves of DNA.[53] The enhancement of the fluorescence intensity is usually ascribed to the higher planarity of the N-methylpiperazine derivative when bound to *ds*-DNA as well as to its protection from collisional quenching.[54,55] If **Ant-PHEA** competes for the same DNA binding sites of Hoechst, a decrease of the fluorescence intensity of the latter must be observed. As depicted in Fig. 4, the fluorescence of the Hoechst-DNA complex is efficiently reduced and 13 nm blue shifted by the addition of the **Ant-PHEA** molecules. Furthermore, the **Ant-PHEA** fluorescence band increases slower after stoichiometry is reached, which is achieved at the same concentration range obtained for the determination of the binding stoichiometry of the **Ant-PHEA**-DNA system shown below, strongly pointing out the outstanding anthracenyl property to displace Hoechst from the adenine and thymine binding sites located in the minor groove, and thus its relatively high affinity towards DNA at least similar to the commercially available probe.

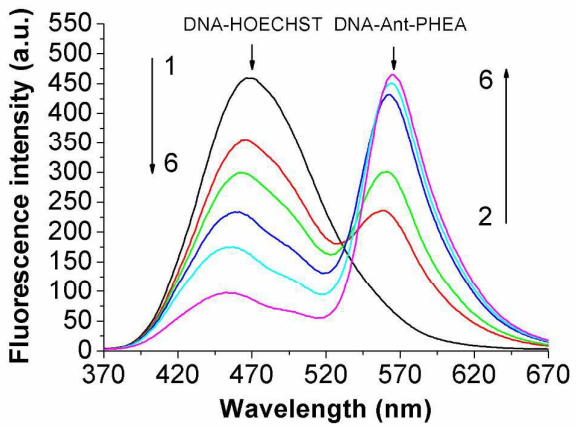

Fig. 4 Fluorescence emission spectra of the competition between Hoechst-DNA complex (λexc: 350 nm) and **Ant-PHEA** treated with: 0.0, 2.5, 5.0, 10., 15.0 and 22.5µM (curves 1-6) of **Ant-PHEA**. $C_{Hoechst}$: 5µM and C_{DNA}: 45 µM.

Additional quantitative information of the fluorescence quenching data were provided by using the Stern-Volmer equation:[56,57]

$$\mathbf{F_0/F = 1 + K_q\,\tau_0\,[Q] = 1 + K_{sv}\,[Q]} \quad (2)$$

Where F_0 and F denote the steady-state fluorescence intensities in the absence and in the presence of quencher (**Ant-PHEA**), respectively. K_{sv} is the Stern-Volmer quenching rate constant, [Q] is the quencher concentration, K_q is the apparent quenching rate constant of the biomolecules and τ_0 is the average excited-state

lifetime of biomolecules without a quencher and it is equal to 10^{-8} s.[57]

From the plot of Equation 2 (Fig. 5), the values of K_{sv} and K_q were obtained and are listed in Table 1.

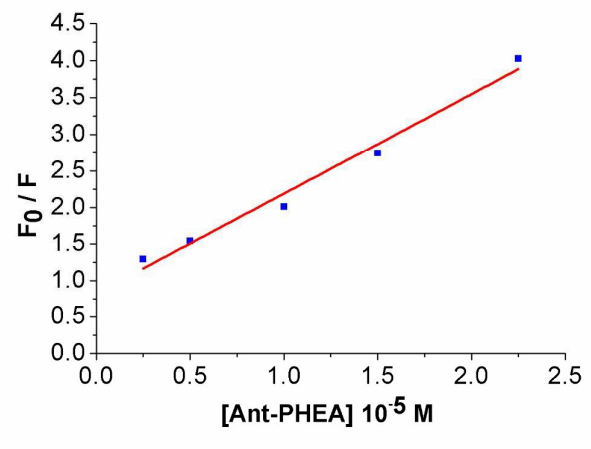

Fig. 5 Stern-Volmer plot for the fluorescence quenching of Hoechst-DNA system by **Ant-PHEA**.

It is well known that the fluorescence quenching can be static, resulting from the formation of a fluorophore-quencher complex or dynamic usually ascribed to the diffusive encounter between the fluorophore and the quencher.[58] Since the value of K_q was much higher than the maximum diffusion collisional quenching rate of various quenchers with biopolymers ≈ 2.0×10^{10} M^{-1} s^{-1} [56,57], the quenching can be ascribed to the formation of **Ant-PHEA**-DNA complex (static) rather than to dynamic collision.[59]

Assuming static quenching the association constant (K_f) and the number of binding sites (n) were analyzed according to the following equation:[60]

$$\log [(F_0 - F)]/F = \log K_f + n \log[Q] \quad (3)$$

The plots of log[(F_0-F)/F] versus log[Q] is linear (Fig. 6) and the values of K_f and n, shown in Table 1, have been obtained from the intercept and the slope, respectively.

Table 1. Stern-Volmer (K_{sv}), quenching rate constant (K_q), association constants (K_f) and number of binding sites (n) of the interaction between **Ant-PHEA** and DNA.

	K_{sv} M^{-1}	K_q M^{-1} s^{-1}	K_f M^{-1}	n
Ant-PHEA	1.36×10^5	1.36×10^{13}	2.0×10^5	1.05

The value of association constant obtained by fluorescence displacement assay agrees well with those found by absorption spectroscopy and it is of the same order of magnitude as that found for Hoechst-DNA complex[61], once again confirming the high binding affinity of the anthracenyl polymer towards the DNA bases (A-T).

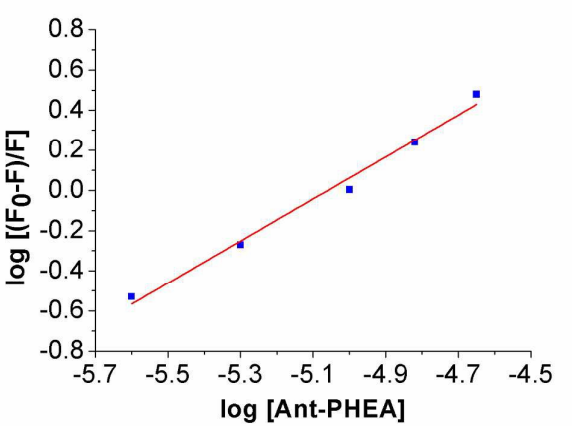

Fig. 6 Plot of log (F_0-F)/F versus log [**Ant-PHEA**].

To provide further insights into the mode of binding of the anthracene derivative towards the DNA moiety, an additional displacement assay was performed by using ethidium bromide as a probe. Ethidium bromide (EB), (3,8-Diamino-5-ethyl-6-phenylphenanthridinium bromide), is well-known intercalator and thus it is often used as a probe to clarify the DNA-binding mode. The increase of the fluorescence intensity of EB upon DNA addition is attributed to the insertion of the planar groups of the drug among the base pairs. If **Ant-PHEA** molecules compete for the same DNA binding sites as EB, a decrease of the fluorescence intensity of the latter must be observed. As depicted in Fig. 7, no appreciable decrease of the fluorescence intensity was observed, thus no displacement of EB occurred, clearly disproving the involvement of an intercalative binding mode.

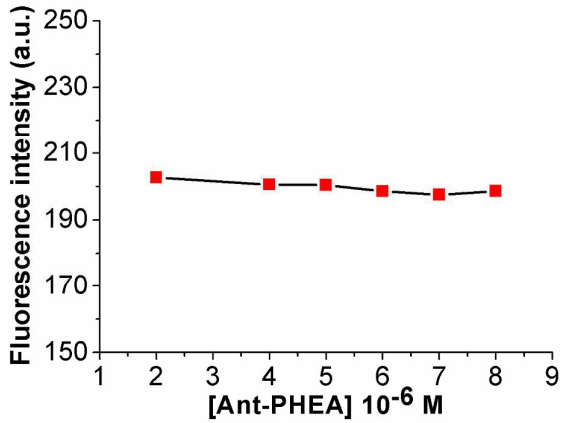

Fig. 7 Fluorescence emission results of the competition between EtBr-DNA complex (λexc: 540 nm) and Ant-PHEA treated with: 2.0, 4.0, 5.0, 6.0, 7.0 and 8.0 μM of **Ant-PHEA**. C_{EtBr} : 5μM and C_{DNA}: 40 μM.

Elucidation of the binding parameters

The binding stoichiometry of **Ant-PHEA** to DNA was evaluated by fluorescence titration using the mole-ratio method, keeping constant the concentration of the DNA and changing that of **Ant-PHEA**. The plot of the variations in fluorescence intensity at 564 nm versus the **Ant-PHEA**/DNA mole ratio is shown in Fig. 8. From the inflection point the molar ratio **Ant-PHEA**/DNA is found to be 0.2, which indicates that one **Ant-PHEA** molecule can interact with five DNA base pairs (bp). The size of the binding site for the classical intercalator ethidium bromide is approximately 2.5 bp[62], whereas the binding site of Hoechst 33258 on DNA is ≈ 5 bp.[53] The value found for **Ant-PHEA** corresponds well to that expected for a minor groove binder[63]; while the large discrepancy with that of the intercalator can be related to the extend arms of the **Ant-PHEA** which establish additional contacts along the groove of the DNA increasing the number of the binding site. This observation also agrees very well with the n value found in the Sterm-Volmer experiment, which suggested that one molecule of Hoechst 33258 was displaced upon binding of one molecule of **Ant-PHEA**.

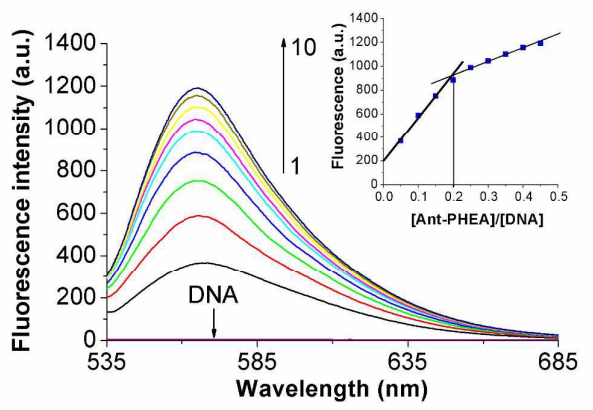

Fig. 8 Fluorescence emission spectra of DNA (50µM) treated with: 0.0, 2.5, 5.0, 7.5, 10.0, 12.5, 15.0, 17.5, 20.0, and 22.5 µM (curves 1-10) of **Ant-PHEA**. Inset: Plot of DNA-**Ant-PHEA** fluorescence intensity vs. the mole ratio.

Melting studies

CD spectroscopy is one of the most common methods employed for the determination of the melting temperature of DNA (T_m) which is defined as the temperature at which half of the total base pairs are unwound. Molecules that bind DNA through intercalation increase the melting temperature by 5-8 °C because they stabilize the double helix structure, while the non-intercalation binding does not cause significant increase in T_m.[64,65] The melting temperature was determined from the transition midpoint of the melting curves of DNA and the **Ant-PHEA**-DNA complex, by monitoring the change in molar ellipticity at 245 nm in the 20-90°C temperature range. The T_m of DNA was found to be 70 °C while a T_m value of 72°C was detected for the **Ant-PHEA**-DNA system, with the DNA/**Ant-PHEA** molar ratio equal to 4 (Fig. 9). These data clearly indicate that **Ant-PHEA** does not intercalate into the DNA base pairs. A similar result was reported in literature for an anthracenyl derivative, which increased the T_m of the CT DNA of 2 °C, and a groove binding mode was assigned.[66] A slight increase in the melting temperature is presumably due to conformational changes of the B-DNA by the insertion of the **Ant-PHEA** within the groove and to its high affinity towards the A-T base pairs, as suggested by the FT-IR and CD spectra discussed further on.

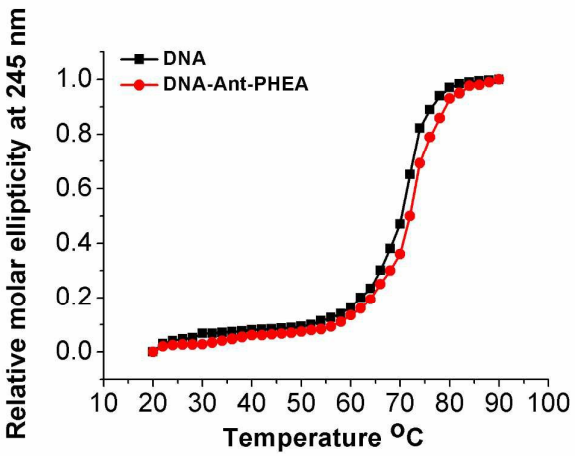

Fig. 9 CD melting profiles of salmon testes DNA in the absence (black line) and presence (red line) of **Ant-PHEA** in 10 mM sodium cacodylate trihydrate (pH 7.25). [DNA] = 40 µM ; [**Ant-PHEA**] = 10 µM.

Fourier transform infrared (FT-IR) spectroscopy

FT-IR spectroscopy is a useful tool to monitor the structural changes generated by the guest molecules in the DNA structure as it provides insights about the sites involved in the interaction.[67] The FT-IR spectra of free salmon testes DNA and the relative structural variations caused by **Ant-PHEA** were studied in aqueous solution (pH 7.25) at different **Ant-PHEA**/DNA molar ratios. The occurrence of the interaction can be deduced by comparing the individual DNA and the **Ant-PHEA** spectra with those of the **Ant-PHEA** / DNA complex (Fig. 10).

The FT-IR spectrum of DNA shows a band at 1655 cm^{-1}, which is attributed to the vibrations of C6=O of guanine (G) and C4=O of thymine (T).[68] The vibrational bands at 1600, 1489,1416 cm^{-1} are typical of adenine (A), cytosine (C), and ring vibrations of guanine (G) bases, respectively.[69] The bands at 1244, 1093, and 968 cm^{-1} are related to the asymmetric and symmetric stretching vibration of phosphate group.[70] Bands with weak relative intensity are located at 834 and 782 cm^{-1} which correspond to the stretching of C-O, P-O (phosphate-ribose diester linkage) and N-H out of plane bending vibrations.[71]

The **Ant-PHEA** FT-IR spectrum presents a strong band at 1730 cm^{-1} that can be assigned to the C=O stretching. Moreover, bands at 1080 and 1166 cm^{-1} could be associated to C-N and C-O stretching, respectively. The bands at 1392, 1450, 1519, and 1602 cm^{-1} are mostly due to C-H bending and C-C stretching of the aromatic rings. A weak intensity band is found at 642 cm^{-1} generated by the C-Br

stretching vibration (residual end group of the short polymer chains).

The **Ant-PHEA**-DNA FT-IR spectra, recorded for solutions with different **Ant-PHEA**/DNA molar ratios are characterized by shifts and intensity variations of the bands relative to the symmetric and asymmetric vibration of phosphate group and of those related to T and A bases (Fig. 11). In particular, in the system with a low **Ant-PHEA**/DNA mole ratio (r=1/8) the asymmetric and symmetric stretching vibration of the phosphate group were shifted from 1244 and 1093 cm^{-1} to 1242 and 1076 cm^{-1}, respectively, and the intensity of the bands at 1655 (T) and 1600 (A) cm^{-1} was reduced and therefore affected by the presence of the ligand. When the molar ratios of **Ant-PHEA** to DNA increased (r=1/5 and r=1/2.5), the band at 1242 cm^{-1} remained unchanged while the band at 1093 cm^{-1} was shifted to 1071 and 1070 cm^{-1}, respectively. In addition, the bands at 1655 cm^{-1} (T) and 1600 cm^{-1} (A) were shifted to 1660 and 1610 cm^{-1}, respectively. It is important to stress that no shift was observed for the bands at 1489 cm^{-1} and 1416 cm^{-1} assigned to cytosine and guanine bases respectively, for each **Ant-PHEA**/DNA molar ratio considered, thus excluding their involvement in the DNA interaction. This behavior brings clear evidence for the existence of interactions between **Ant-PHEA** and DNA, occurring through the main contribution of the phosphate groups and the A and T bases. Spectral changes observed here clearly establish that the **Ant-PHEA**-DNA adduct is manly stabilized by hydrophobic forces since the DNA bases, in particular thymine and adenine, are involved in the complexation process while suggesting a further (though minor) adduct stabilization through van der Waals forces and hydrogen bonding arising due to surface binding between the hydrophilic polymeric arms of the ligand and the specific functional groups positioned on the edge of DNA bases (bottom groove region). It is worth noting that the insertion of the ligand in the DNA groove can destabilize the B-DNA form to some degree, in agreement with the CD data discussed further on, therefore leading to distortion and perturbation on the phosphate-sugar backbone located in the wall groove region. Typically groove binders show a high affinity for the areas rather rich in adenine and thymine and the choice of selective placement of electronegative atoms determines the DNA binding profile. On the other hand, guanine and cytosine sequences get unstacked easily and intercalation preferentially occurs in that area.[72]

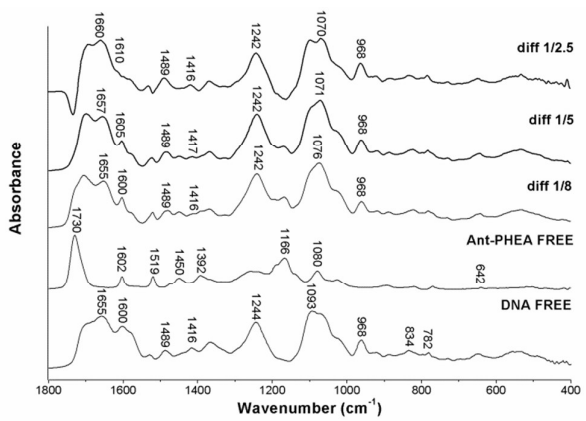

Fig. 10 FT-IR spectra and difference FT-IR spectra [(DNA solution + **Ant-PHEA** solution) – **Ant-PHEA** solution] of the free DNA and DNA-**Ant-PHEA** complex at different molar ratios in the 1800-400 cm^{-1} region.

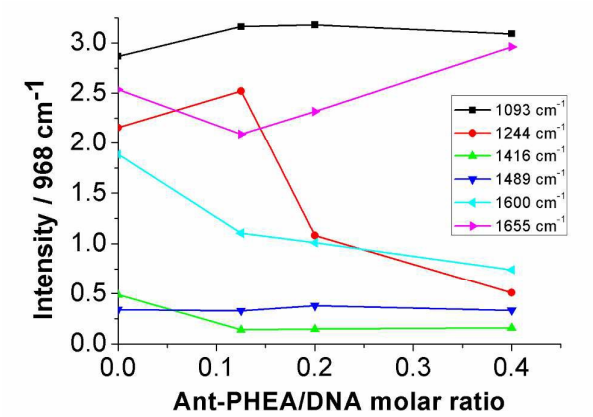

Fig. 11 Intensity ratio variations as a function of **Ant-PHEA** concentration.

Thermodynamic studies

The binding between guest molecules and DNA can involve hydrogen bonds, van der Waals forces, electrostatic and hydrophobic interactions. The thermodynamic parameters, such as the entropic and enthalpic contributions to the whole binding process, are good indicators to establish which type of interaction regulates the association between small molecules and DNA. Positive values of enthalpy and entropy can be ascribed to hydrophobic interaction, whereas negative values of both enthalpy and entropy indicate Van der Waals forces or hydrogen bond formation.[73] We calculated the thermodynamic parameters using the K_a values determined in 3.1, by applying the equation:[74-76]

$$\log K_a = -\frac{\Delta H^0}{2.303RT} + \frac{\Delta S^0}{2.303R} = -\frac{\Delta G^0}{2.303RT} \quad (4)$$

The values of ΔH^0 and ΔS^0 were determined from the slope and the intercept of the linear plot between log K_a and the reciprocal absolute temperature (Fig. 12). The negative values of ΔG^0 (-31.44, -33.00 and -34.55 kj mol^{-1} at 298, 304 and 310 K, respectively) clearly indicate the spontaneity of the process. Both ΔH^0 (45.70 kj mol^{-1}) and ΔS^0 (258.87 j mol^{-1} K^{-1}) being positive indicates that the **Ant-PHEA**-DNA complex is stabilized mainly by hydrophobic interactions even though hydrogen bonding and van der Waals forces cannot be excluded.[73] Similar results are also found for groove binders such as emodin, methyldopa and thiabendazole.[48,77,78] Moreover, it has been reported that complex formation between DNA and synthetic macromolecules such as poly(ethylene glycol) (PEG) and dendrimers can be ascribed to the stabilization induced by hydrophobic interactions *via* polymer aliphatic chain and hydrophobic groove's region.[79,80]

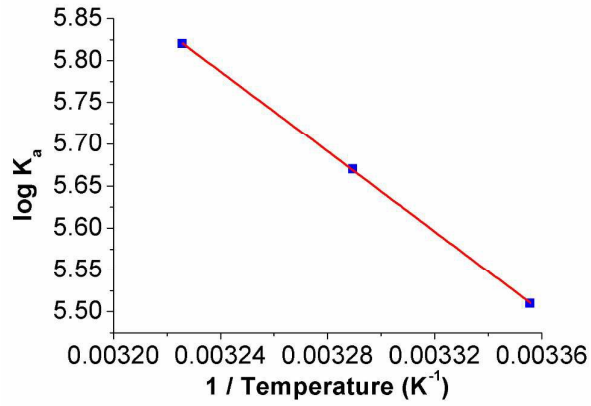

Fig. 12 Van't Hoff plot for the binding of **Ant-PHEA** to DNA.

Circular Dichroism spectral studies

In order to evaluate if **Ant-PHEA** promotes conformational changes to DNA, circular dichroism (CD) spectroscopy was applied. The measurements were performed at 298 and 313 K. The B-DNA form is characterized by a positive CD band at about 260-280 nm due to base stacking and a negative band around 245 nm due to right-handed helicity, the exact positions of the CD bands depending strongly on the sequence diversity.[81,82] **Ant-PHEA**, which is achiral, is thus optically inactive. However, upon interaction with DNA an induced circular dichroism (ICD) band appears around 320 nm, resulting from the coupling of the electric transition moments of the ligand and the DNA bases. A positive ICD signal is found usually for ligands bound to the groove of B-DNA, whereas negative or bisignate ICD bands are expected for intercalators.[83,84] The presence of a single positive ICD signal in the region between 300-330 nm is an immediate proof that **Ant-PHEA** binds to DNA and an indication that the interaction takes place in the groove. In order to better elucidate the binding mode, the positive and negative DNA bands, which are highly sensitive to the interaction with guest molecules, were analyzed (Fig. 13). A decrease of both bands was observed upon **Ant-PHEA** addition. Intercalation of aromatic chromophore results in enhancement of the positive band while the negative CD band can be altered in various ways depending of the orientation of the ligand inside the intercalation site. Molecules which intercalate perpendicular to the base pairs, such as daunomycin[85], induce a decrease of the intensity of the 245 nm band, whereas molecules interacting with their chromophores parallel to base pairs, such as ethidium bromide[86] and proflavin[87], lead to an increase of the intensity of the negative CD band. On the other hand, guest molecules interacting with the groove, such as berenil[88], were found to decrease both the DNA CD bands. The intensity of the 278 nm band, recorded at 298 K, in native DNA was found to be 6.75 mdeg. After the addition of **Ant-PHEA**, a linear decrease was observed leading to a value of 6.04 mdeg without any significant shift of the band. The negative band at 245 nm seems to be less affected in the presence of **Ant-PHEA** with a total change of 0.34 mdeg. A different trend was observed at 313 K, since the band at 278 nm gives rise to a total change in ellipticity of 0.21 mdeg while the negative band at 245 nm shows a decrease in intensity of 0.75 mdeg pointing out a destabilization of the DNA helix to some extent. Nevertheless, even if a slight destabilization of the B-DNA secondary structure occurs upon ligand binding the biopolymer still remains in the B-family conformation and no DNA aggregation can be detected. Similar magnitude of change was found in some groove binders, e.g. furamidine, netropsin and distamycin.[89,90] Further, both the CD spectra presented an isoelliptic point at 252 nm, revealing the formation of a complex between the guest and host molecules. The CD data confirm that the interaction between **Ant-PHEA** and DNA is affected by temperature and that the guest molecule interacts with the groove of the DNA.

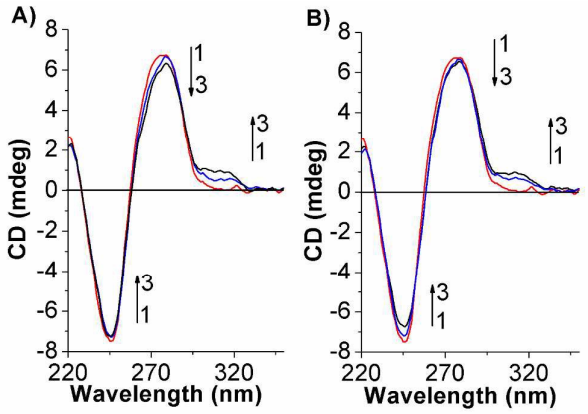

Fig. 13 Circular dichroism (CD) spectra of DNA (50.0 μM) treated with: 0.0, 15.0 and 30.0 μM (curves 1-3) of **Ant-PHEA** at 298 (A) and 313 (B) K.

Effect of ionic strength

The effect of ionic strength on the interaction between **Ant-PHEA** and DNA was determined by monitoring the fluorescence intensity at 564 nm on solutions in which the ionic strength was modified using NaCl concentration in the range from 0 to 1.0 M. As reported in section 3.2, upon the addition of DNA the fluorescence intensity of **Ant-PHEA** increases significantly. It was observed that NaCl leads to a decrease of the fluorescence intensity by 5%, and further addition of the salt did not change the intensity of the band. This variation is marginal, indicating that phosphonate screening does not hinder much the association process, in consistency with what had been suggested by other experiments. . This result could be expected in regard with the neutral nature of the polymer chain, which limits the interaction with anionic phosphate substituents; conversely, this suggests that substituting the pendant neutral group on the polymer side chain by cationic moieties could be a relevant strategy in order to enhance binding affinities of fluorescent probes towards DNA.[91]

Conclusions

The DNA-binding properties of an anthracenyl polymer derivative (**Ant-PHEA**) have been comprehensively studied by various methods including UV-Vis, fluorescence, FT-IR and

circular dichroism. The data obtained by UV-Vis and fluorescence studies indicate that **Ant-PHEA** interacts with DNA via groove binding mode. In particular, competition experiments with Hoechst and EtBr constitute a firm evidence for this binding mode, and clearly rule out intercalation. The 1:5 **Ant-PHEA**:DNA interaction stoichiometry highlights that most sites of DNA participate in the association process. FT-IR spectra indicate that the sites, involved to a greater extent, are the phosphate groups and adenine and thymine bases. The negative values of ΔG^0 confirm the spontaneity of the process, while the values of $\Delta H>0$ and $\Delta S>0$ show that hydrophobic forces regulate the binding of the **Ant-PHEA** with DNA. Circular dichroism spectra reveal partial modification on DNA structure confirming the groove binding mode. These small changes of the DNA secondary structure are supported by the melting temperature studies, which show a modification of T_m by only 2°C, which is perfectly in line with the proposed groove binding mode. These results clearly establish the potential of **Ant-PHEA** to be used as a DNA groove binder, and constitutes an advantageous substitute to some currently commercially available probes, such as Hoechst 33258. The resulting **Ant-PHEA** / DNA composite material could be a valuable candidate for future photonics and/or biological applications.

Acknowledgements

The financial support from NCN OPUS project DEC-2013/09/B/ST5/03417 and a statutory activity subsidy from the Polish Ministry of Science and Higher Education for the Faculty of Chemistry of WUT are acknowledged.

Notes and references

1 M. Pawlicki, H. A. Collins, R. G. Denning and H. L. Anderson, *Angew. Chem. Int. Ed. Engl.*, 2009, **48**, 3244.
2 J. R. G. Navarro, F. Lerouge, C. Cepraga, G. Micouin, A. Favier, D. Chateau, M. –T. Charreyre, P. –H. Lanoë, C. Monnereau, F. Chaput, S. Marotte, Y. Leverrier, J. Marvel, K. Kamada, C. Andraud, P. L. Baldeck and S. Parola, *Biomaterials*, 2013, **34**, 8344.
3 J. Olesiak-Bańska, H. Mojzisova, D. Chauvat, M. Zielinski, K. Matczyszyn, P. Tauc, and J. Zyss, *Biopolymers*, 2011, **95**, 365.
4 H. Mojzisova, J. Olesiak, M. Zielinski, K. Matczyszyn, D. Chauvat and J. Zyss, *Biophys. J.*, 2009, **97**, 2348.
5 J. Olesiak-Bańska, K. Matczyszyn, R. Zaleśny, N. A. Murugan, J. Kongsted, H. Agren, W. Bartkowiak and M. Samoć, *J. Phys. Chem. B.*, 2013, **117**, 12013.
6 J. Olesiak-Bańska, P. Hańczyc, K. Matczyszyn, B. Norden and M. Samoć, *Chem. Phys.*, 2012, **404**, 33.
7 G. S. He, L. –S. Tan, Q. Zheng and P. N. Prasad, *Chem. Rev.*, 2008, **108**, 1245.
8 C. Monnereau, S. Marotte, P. H. Lanoë, O. Maury, P. L. Baldeck, D. Kreher, A. Favier, M. T. Charreyre, J. Marvel, Y. Leverrier and C. Andraud, *New J. Chem.*, 2012, **36**, 2328.
9 J. Massin, A. Charaf-Eddin, F. Appaix, Y. Bretonniere, D. Jacquemin, B. van der Sanden, C. Monnereau and C. Andraud, *Chem. Sci.*, 2013, **4**, 2833.
10 J. Massin, S. Parola, C. Andraud, F. Kajzar and I. Rau, *Optical Materials*, 2013, **35**, 1810.
11 E. M. Heckman, J. G. Grote, F. K. Hopkins and P. P. Yaney, *Appl. Phys. Let.*, 2006, **89**, 181116.
12 J. G. Grote, J. A. Hagen, J. S. Zetts, R. L. Nelson, D. E. Diggs, M. O. Stone, P. P. Yaney, E. Heckman, C. Zhang, W. H. Steier, A. K. –Y. Jen, L. R. Dalton, N. Ogata, M. J. Curley, S. J. Clarson and F. K. Hopkins, *J. Phys. Chem. B*, 2004, **108**, 8584.
13 Y. W. Kwon, D. H. Choi and J. I. Jin, *Polym. J*, 2012, **44**, 1191.
14 K. Matczyszyn and J. Olesiak-Bańska, *J Nanophotonics* 2012, **6**, 064505.
15 F. Ciardelli, M. Bertoldo, S. Bronco, A. Pucci, G. Ruggeri and F. Signori, *Polym. Int*, 2013, **62**, 22.
16 N. Nakamoto, M. Tsuboi and G. D. Strahan, *Methods Biochem. Anal.*, 2008, **51**, 1.
17 M. Sirajuddin, S. Ali and A. Badshah, *J. Photochem. Photobiol., B.*, 2013, **124**, 1.
18 M. Demeunynck, C. Bailly and W. D. Wilson, (Eds.). Wiley-VCH. 2002, Weinheim.*
19 P. B. Dervan, *Science*, 1986, **232**, 464.
20 P. B. Dervan, Bioorg. *Med. Chem.*, 2001, **9**, 2215.
21 C. Bailly and J. B. Chaires, *Bioconjugate Chem.*, 1998, **9**, 513.
22 C. V. Kumar, E. H. Punzalan and W. B. Tan, *Tetrahedron.*, 2000, **56**, 7027.
23 S. Neidle, *Nut. Prod. Rep.*, 2001, **18**, 291.
24 H. Ihmels and D. Otto, *Top Curr Chem.*, 2005, **258**, 161.
25 L. H. Hurley, *Nat Rev Cancer.*, 2002, **2**, 188.
26 B. C. Baguley, *Anti-Cancer Drug Des.*, 1991, **6**, 1.
27 S. Nafisi, A. A. Saboury, N. Keramat, J. F. Neault and H. -A Tajmir-Riahi, *J. Mol. Struct.* 2007, **827**, 35.
28 A. Paul and S. Bhattacharya, *Curr. Sci.*, 2012, **102**, 212.
29 S. Kumar, P. Pandya, K. Pandav, S. P. Gupta and A. Chopra, *J. Biosci.*, 2012, **37**, 553.
30 R. E. Dickerson and H. R. Drew, *J. Mol. Biol.*, 1981, **149**, 761.
31 F. J. Meyer-Almes and D. Porschke, *Biochemistry*, 1993, **32**, 4246.
32 W. B. Tan, A. Bhambhani, M. R. Duff, A. Rodger and C. V. Kumar, *Photochem. Photobiol.*, 2006, **82**, 20.
33 J. Marmur, *J. Mol. Biol.*, 1961, **3**, 208.
34 N. Raman, S. Sobha and M. Selvaganapathy, *Monatsh Chem.*, 2012, **143**, 1487.
35 J. F. Neault and H. A. Tajmir Riahi, *J. Phys. Chem.B.*, 1998, **102**, 1610.
36 J. F. Neault and H. A. Tajmir Riahi, *J. Biol. Chem.*, 1996, **271**, 8140.
37 Sh. Nafisi, A. Sobhanmanesh, K. Alimoghaddam, A. Ghavamzadeh and H. A. Tajmir-Riahi, *DNA cell Biol.*, 2005, **24**, 634.
38 D. Banerjee and S. K. Pal, *J. Phys. Chem. B*, 2007, **111**, 10833.
39 H. Sun, J. Xiang, Y. Liu, L. Li, Q. Li, G. Xu and Y. Tang, *Biochimie*, 2011, **93**, 1351.
40 J. Jaumot and R. Gargallo, *Curr. Pharmaceut. Des.*, 2012, **18**, 1900.
41 K. Bhadra and G. S. Kumar, *Biochim. Biophys. Acta.*, 2011, **1810**, 485.
42 M. Deiana, K. Matczyszyn, J. Massin, J. Olesiak-Banska, C. Andraud and M. Samoc, *PLoS ONE* 2015, **10**, e0129817.
43 J. Liu, T. Zhang, T. Lu, L. Qu, H. Zhou, Q. Zhang and L. Ji, *J. Inorg. Biochem.*, 2002, **91**, 269.
44 S. Dey, S. Sarkar, H. Paul, E. Zangrando and P. Chattopadhyay, *Polyhedron*, 2010, **29**, 1583.
45 K. A. Kumar, K. L. Reddy, S. Vidhisha and S. Satyanarayana, *Appl. Organometal. Chem.*, 2009, **23**, 409.
46 G. Pratviel, J. Bernadou and B. Meunier, *Adv. Inorg. Chem.* 1998, **45**, 251.
47 N. Shahabadi, S. Kashanian, M. Khosravi and M. Mahdavi, *Tran. Met. Chem.*, 2010, **35**, 699.
48 S. Bi, H. Zhang, C. Qiao, Y. Sun and C. Liu, *Spectrochim. Acta, Part A.*, 2008, **69**, 123.

49 T. Sarwar, M. A. Husain, S. U. Rehman, H. M. Ishqi and M. Tabish, *Mol. BioSyst.*, 2015, **11**, 522.
50 S. S. Kalanur, U. Katrahalli and J. Seetharamappa, *J. Electroanal. Chem.*, 2009, **636**, 93.
51 Y. G. Guo, J. B. Chao and J. H. Pan, *Spectrochim. Acta. Part A.*, 2007, **68**, 231.
52 H. A. Benesi and J. H. Hildebrand, *J. Am. Chem. Soc.*, 1949, **71**, 2703.
53 P. E. Pjura, K. Grzeskowiak and R. E. Dickerson, *J. Mol. Biol.*, 1987, **197**, 257.
54 Y. Guan, W. Zhou and X. Yao, *Anal. Chim. Acta.*, 2006, **570**, 21.
55 R. Lavery and B. Pullman. *Nucleic Acids Res.*, 1981, **9**, 3765.
56 J. K. Lakowicz, Principles of Fluorescence Spectroscopy, second ed. Plenum Press, New York. 1999.
57 T. G. Dewey (Ed.), Biophysical and Biochemical Aspects of Fluorescence Spectroscopy, Plenum Press, New York. 1991, 1.
58 M. Mansouri, M. Pirouzi, M. R. Saberi, M. Ghaderabad and J. Chamani, *Molecules*, 2013, **18**, 789.
59 P. S. Dorraji and F. Jalali, *J. Braz. Chem. Soc.*, 2012, **24**, 939.
60 M. Shakir, M. Azam, S. Parveen, A. U. Khan and F. Firdaus, *Spectrochim. Acta A.*, 2009, **71**, 1851.
61 R. Sarkar and S. K. Pal *Biomacromolecules*, 2007, **8**, 3332.
62 A. I. Dragan, R. Pavlovic, J. B. McGivney, J. R. Casas-Finet, E. S. Bishop, R. J. Strouse, M. A. Schenerman and C. D. Geddes, *J. Fluoresc.* 2012, **22**, 1189.
63 Y. Shi, C. Guo, Y. Sun, Z. Liu, F. Xu, Y. Zhang, Z. Wen and Z. Li, *Biomacromolecules*, 2011, **12**, 797.
64 Y. J. Liu, X. Y. Wei, F. H. Wu, W. J. Mei and L. X. He, *Spectrochim. Acta. A: Mol. Biomol. Spectrosc.*, 2008, **70**, 171.
65 C. Y. Qiao, S. Y. Bi, Y. Sun, D. Q. Song, H. Q. Zhang and W. H. Zhou, *Spectrochim. Acta. A: Mol. Biomol. Spectrosc.* 2008, **70**, 136.
66 Y. Huang, Y. Zhang, J. Zhang, D. W. Zhang, Q. S. Lu, J. L. Liu, S. Y. Chen, H. H. Lin and X. Q. Yu, *Org. Biomol. Chem.*, 2009, **7**, 2278.
67 H. Morjani, J. F. Riou, I. Nabiev, F. Lavalle and M. Manfait, *Cancer res.*, 1993, **53**, 4784.
68 M. B. James, A. W. Michael and J. T. George, *Biochemistry*, 1991, **30**, 8918.
69 K. Senthil and R. Sarojini, *Int J Biochem Biotechnol.*, 2009, **5**, 251.
70 E. V. Hackl, S. V. Kornilova, L. E. Kapinos, V. V. Andrushchenko, V. L. Galkin, D. N. Grigoriev and Y. P. Blagoi, *J. Mol. Struct.*, 1997, **229**, 408.
71 B. Rafique, A. M. Khalid, K. Akhtar and A. Jabbar, *Biosens Bioelectron.*, 2013, **44**, 21.
72 A. Paul and S. Bhattacharya, *Curr. Sci.*, 2012, **102**, 212.
73 P. D. Ross and S. Subramanian, *Biochemistry*, 1981, **20**, 3096.
74 N. Zhao, X. M. Wang, H. Z. Pan, Y. M. Hu and L. S. Ding, *Spectrochim. Acta, Part A.*, 2010, **75**, 1435.
75 M. Ortiz, A. Fragosoa, P. J. Ortiz and C. K. O'Sullivan, *J. Photochem. Photobiol. A.*, 2011, **218**, 26.
76 X. L. Li, Y. J. Hu, H. Wang, B. Q. Yu and H. L. Yue, *Biomacromolecules*. 2012, **13**, 873.
77 N. Shahabadi and M. Maghsudi, *Mol. BioSyst.*, 2014, **10**, 338.
78 F. Jalali and P. S. Dorraji, *Arab. J. Chem.*, 2014, In Press.
79 E. Froehlich, J. S. Mandeville, C. M. Weinert, L. Kreplak and H. A. Tajmir-Riahi, *Biomacromolecules*, 2011, **12**, 511.
80 E. Froehlich, J. S. Mandeville, D. Arnold, L. Kreplak and H. A. Tajmir-Riahi, *J. Phys. Chem. B*, 2011, **115**, 9873.
81 H. C. Nelson, J. T. Finch, B. F. Luisi and A. Klug, *Nature*, 1987, **330**, 221.
82 D. G. Alexeev, A. A. Lipanov and I. Skuratovskii, *Nature*, 1987, **325**, 821.
83 G. A. Ellestad, Drug and Natural Product Binding to Nucleic Acids Analyzed by Electronic Circular Dichroism, in Comprehensive Chiroptical Spectroscopy: Applications in Stereochemical Analysis of Synthetic Compounds, Natural Products, and Biomolecules, Volume 2 (eds N. Berova, P. L. Polavarapu, K. Nakanishi and R. W. Woody), John Wiley & Sons, Inc., Hoboken, NJ, USA. 2012.
84 N. C. Garbett, P. A. Ragazzon and J. B. Chaires, *Nature Protocols*, 2007, **2**, 3166.
85 C. A. Frederick, L. D. Williams, G. Ughetto, G. A. van der Martel, J. H. van Boom, A. Rich and A. H. J. Wang, *Biochemistry*, 1990, **29**, 2538.
86 E. Slobodyansky, J. Stellwagen and N. C. Stellwagen, *Biopolymers*, 1998, **27**, 1107.
87 G. T. Walker, M. P. Stone and T. R. Krugh, *Biochemistry*, 1985, **24**, 7471.
88 M. V. Gonzàlez, P. Amo-Ochoa, J. M. Pérez, M. A. Fuertes, J. R. Masaguer, C. Navarro-Ranninger and C. Alonso, *J Inorg Biochem*, 1996, **63**, 57.
89 G. A. Ellestad, *Natural Prod. Biomol.*, 2012, **2**, 635. (John Wiley & Sons).
90 C. A. Laughton, F. Tanious, C. M. Nunn, D. W. Boykin, W. D. Wilson and S. Neidle, *Biochemistry*, 1996, **35**, 5655.
91 H. Srour, O. Ratel, M. Leocmach, E. A. Adams, S. Denis-Quanquin, V. Appukuttan, N. Taberlet, S. Manneville. J. –C. Majesté, C. Carrot, C. Andraud and C. Monnereau, *Macromol Rapid Commun.*, 2015, **36**, 55.

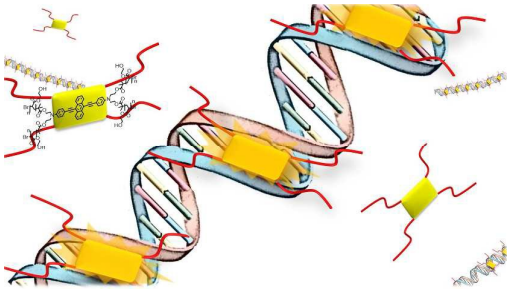

Graphical abstract.